

**Dieses Dokument ist eine Zweitveröffentlichung (Postprint) /
This is a self-archiving document (accepted version):**

R. Hentschel, J. Gärtner, A. Wachowiak, A. Großer, T. Mikolajick, S. Schmult

Surface morphology of AlGaN/GaN heterostructures grown on bulk GaN by MBE

Erstveröffentlichung in / First published in:

Journal of Crystal Growth. 2018, 500, S. 1-4 [Zugriff am: 10.10.202]. Elsevier. ISSN 0022-0248.

DOI: <https://doi.org/10.1016/j.jcrysgro.2018.07.026>

Diese Version ist verfügbar / This version is available on:

<https://nbn-resolving.org/urn:nbn:de:bsz:14-qucosa2-811804>



Dieses Werk ist lizenziert unter einer [Creative Commons Namensnennung – Nicht kommerziell – Keine Bearbeitungen 4.0 International Lizenz](https://creativecommons.org/licenses/by-nc-nd/4.0/).

This work is licensed under a [Creative Commons Attribution-NonCommercial-NoDerivatives 4.0 International License](https://creativecommons.org/licenses/by-nc-nd/4.0/).

Accepted Manuscript

Surface morphology of AlGa_N/Ga_N heterostructures grown on bulk Ga_N by MBE

R. Hentschel, J. Gärtner, A. Wachowiak, A. Großer, T. Mikolajick, S. Schmult

PII: S0022-0248(18)30334-8
DOI: <https://doi.org/10.1016/j.jcrysgr.2018.07.026>
Reference: CRYG 24680

To appear in: *Journal of Crystal Growth*

Received Date: 8 June 2018
Revised Date: 20 July 2018
Accepted Date: 25 July 2018

Please cite this article as: R. Hentschel, J. Gärtner, A. Wachowiak, A. Großer, T. Mikolajick, S. Schmult, Surface morphology of AlGa_N/Ga_N heterostructures grown on bulk Ga_N by MBE, *Journal of Crystal Growth* (2018), doi: <https://doi.org/10.1016/j.jcrysgr.2018.07.026>

This is a PDF file of an unedited manuscript that has been accepted for publication. As a service to our customers we are providing this early version of the manuscript. The manuscript will undergo copyediting, typesetting, and review of the resulting proof before it is published in its final form. Please note that during the production process errors may be discovered which could affect the content, and all legal disclaimers that apply to the journal pertain.



Surface morphology of AlGa_N/Ga_N heterostructures grown on bulk Ga_N by MBE

Corresponding Author: Rico Hentschel

R. Hentschel¹, J. Gärtner¹, A. Wachowiak¹, A. Großer¹, T. Mikolajick^{1,2} and S. Schmult²

¹ Namlab gGmbH, Noethnitzer Str. 64, 01187 Dresden, Germany

² TU Dresden, Institute of Semiconductors and Microsystems, Noethnitzer Str. 64, 01187 Dresden, Germany

Electronic mail: Rico.Hentschel@namlab.com

Keywords: A3. Molecular Beam Epitaxy; B1. Gallium nitride; A1. Surface morphology; A1. Atomic force microscopy; B3. AlGa_N/Ga_N heterostructure

In this report the influence of the growth conditions on the surface morphology of AlGa_N/Ga_N heterostructures grown on sapphire-based and bulk Ga_N substrates is nondestructively investigated with focus on the decoration of defects and the surface roughness. Under Ga-rich conditions specific types of dislocations are unintentionally decorated with shallow hillocks. In contrast, under Ga-lean conditions deep pits are inherently formed at these defect sites. The structural data show that the dislocation density of the substrate sets the limit for the density of dislocation-mediated surface structures after MBE overgrowth and no noticeable amount of surface defects is introduced during the MBE procedure. Moreover, the transfer of crystallographic information, e.g. the miscut of the substrate to the overgrown structure, is confirmed. The combination of our MBE overgrowth with the employed surface morphology analysis by atomic force microscopy (AFM) provides a unique possibility for a nondestructive, retrospective analysis of the original substrate defect density prior to device processing.

1. Introduction

Remarkable performance of GaN-based power devices has been demonstrated during the last years, driven by the technological advancements in lateral device technology¹⁻⁵. Crucial for the operation of high electron mobility transistors (HEMTs) typically used for radio frequency or power electronics applications is a flat and smooth surface and a well-defined AlGaIn/GaN interface to achieve a high two-dimensional electron gas (2DEG) mobility^{6,7}.

In this report the impact of structural substrate properties as well as the stoichiometry during MBE growth on the surface morphology of functional AlGaIn/GaN heterostructures is discussed. Motivated by previous reports^{8,9} the obtained morphology data of MBE layers grown on sapphire-based substrates and bulk GaN having a threading dislocation density that changes by 5 orders of magnitude are compared. Spatial variations in the III/N-ratio during the MBE growth allow to change the morphological appearance on one wafer and in one growth run. Investigations of the sample surfaces by atomic force microscopy (AFM) before and after heterostructure growth reveal, that the inherent decoration of defects strongly depends on the III/N stoichiometry (as already known from previous work^{10,11}), whereas its impact on the surface morphology depends on the dislocation density. For dislocation-lean substrates the sensitivity to the III/N ratio is not visible. Our results imply that the defect density of characteristic surface features is predominantly defined by the used substrate.

2. Experimental

Sections 2.1, 2.2 and 2.3 describe in detail the growth and characterization procedures of the fabricated structure shown in Fig. 1.

2.1 Specifications of the used Templates

In this study c-axis, Ga-polar and epitaxy-ready two inch templates and substrates were utilized as starting material for subsequent growth of wurtzite AlGaN/GaN heterostructures. The templates originate from metal-organic vapor phase epitaxy (MOVPE) as well as hydride vapor phase epitaxy (HVPE) on sapphire. The thickness of the GaN layers ranges from 2 μm to 90 μm , resulting in densities between $2 \cdot 10^8 \text{ cm}^{-2}$ and $3 \cdot 10^9 \text{ cm}^{-2}$ for screw and mixed-type dislocations, respectively^{12,13}. The 650 μm thick bulk GaN substrate originates from an ammonothermal growth process with a vendor specified etch-pit density related to dislocations of less than $5 \cdot 10^4 \text{ cm}^{-2}$. The root mean square roughness R_{RMS} for all used templates was determined to be below 0.6 nm by AFM before the MBE overgrowth, which will be described in the following section.

2.2 Growth of the MBE AlGaN/GaN heterostructure

The growth was performed in a VG 80H plasma-assisted MBE system (base pressure $< 10^{-10}$ Torr). Prior to the MBE step all wafers and templates were out-gassed in an ultra-high vacuum environment (UHV) at $> 500 \text{ }^\circ\text{C}$ for at least 4 hours and transferred into the growth chamber under UHV conditions. Metals with a purity of 8N for gallium and 6N5 for aluminum were evaporated from single-filament effusion sources and active nitrogen (10N) was supplied by an RF-plasma source. The samples are grown at a temperature approximately 10 K below the rapid thermal desorption point for Ga on the wafer surface and result in a deposition rate of 240 nm/h and 2D growth mode of intrinsic

material as reported elsewhere^{14,15}. The layer stack consists of a 1 μm thick GaN layer, followed by a 16 nm thick $\text{Al}_{0.06}\text{Ga}_{0.94}\text{N}$ barrier layer and a 3 nm thick GaN cap (see Fig. 1). The 2DEG is formed at the GaN/AlGaN interface and the layer architecture results in electron densities of around $2 \cdot 10^{12} \text{ cm}^{-2}$ ^{16,17}. For the interpretation of the surface morphology data it is important to know that under the applied sample rotation the Ga/N-ratio exhibits a drop of 2 % the wafer center towards the edge, which was extracted from thickness variations over the wafer. This inhomogeneity allows for Ga-rich stoichiometry in the wafer center and Ga-lean conditions towards the wafer edge in a single growth run.

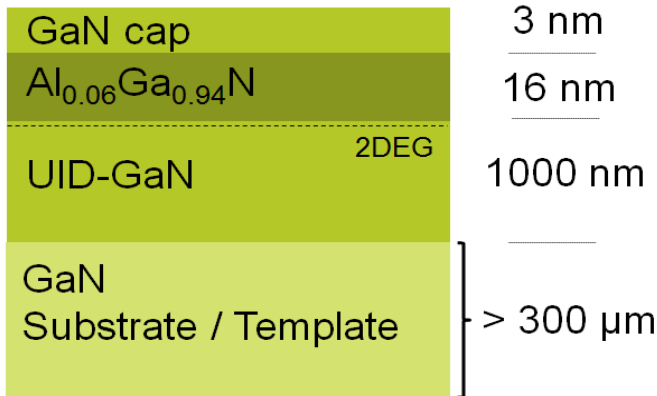


Fig. 1: Schematic cross-section of the AlGaN/GaN heterostructure capped with a 3 nm GaN layer. All MBE layers were grown without any intentional doping on the different GaN substrates / templates originating from VPE or ammonothermal processes.

2.3 Structural characterization

The sample surface morphology has routinely been investigated before and after the MBE step with a Digital Instruments Dimension 3100 atomic force microscope. The dislocation density of the material was estimated from evaluating the density of visible surface defects. Their decoration during the MBE growth is characteristic and depends on the III/N ratio.

3. Results and discussion

In this section the influence of the III/N ratio on the surface morphology is discussed in detail. Initially the epi-ready surfaces were analyzed to determine or verify the surface defect density and roughness. Finally, the morphology after the MBE growth on the different substrates has been examined. For all micrographs an area of $5 \times 5 \mu\text{m}^2$ was scanned. Line profiles were locally extracted from the data in order to compare the different morphologies on a smaller lateral scale.

3.1 Morphology data of the sapphire-based GaN substrates

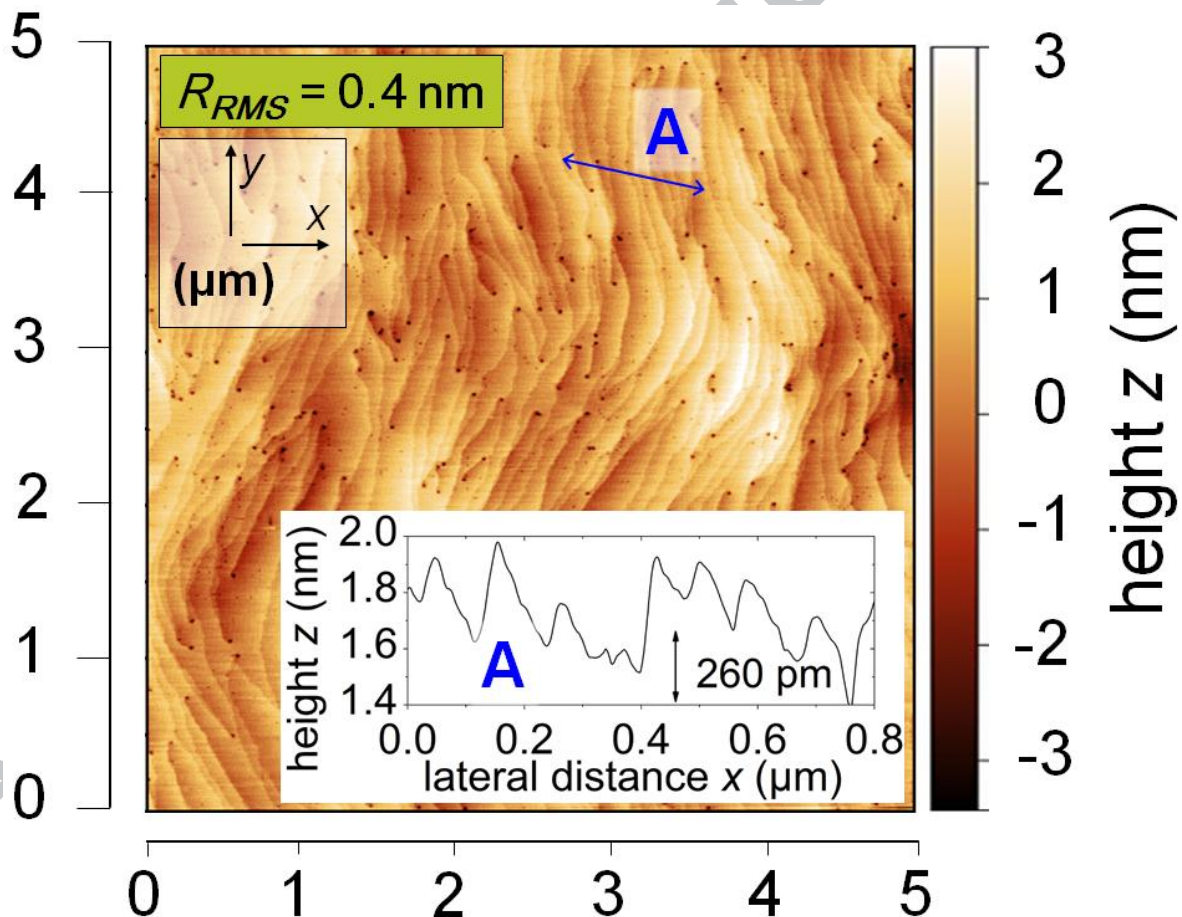


Fig. 2: Surface morphology of a common as-grown VPE template on sapphire, prior to the MBE overgrowth. A stepped-terraces structure and pit-like defects with a depth of 1 nm - 2 nm are observable. The line scan profile A shows the height of the terrace step edges with one (260 pm) or two atomic layers per step (lattice constant in c-direction: 518 pm).

A typical AFM image and line profile taken on a thin MOVPE grown GaN layer on sapphire before the MBE growth is presented in Fig. 2. A smooth surface with terraces of mono- or bilayer high step edges and a $R_{RMS} < 0.5$ nm is observed. Pits of 1 nm - 2 nm depth located at the termination point of terrace step edges and with a density of around $2 \cdot 10^9$ cm⁻² mark threading screw dislocations (TSD) and mixed type dislocations (TMD)¹⁸. Even shallower pits (< 1nm depth) often aligned along lines are resolved on terraces away from step edges related to endpoints of threading edge dislocations (TED). The morphology of the same surface after the MBE overgrowth under Ga-lean conditions is

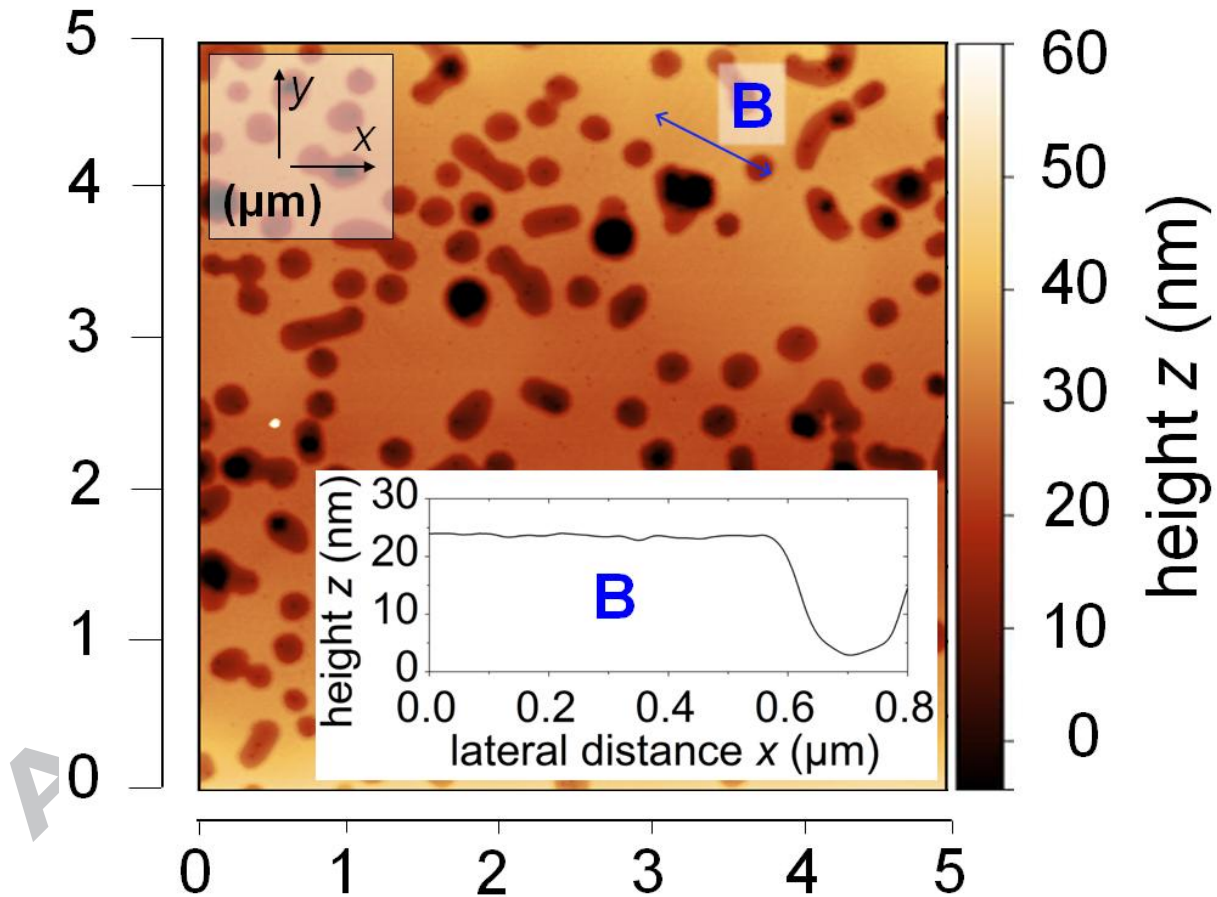


Fig. 3: Surface morphology of an MBE-grown layer under Ga-lean conditions taken 10 mm from the edge of the substrate. Dislocations in the MBE material result in the formation of deep pits at the surface. The monolayer terrace structure is observed in the flat regions between the pits. The line scan profile B shows an example of the pit depth.

displayed in Fig. 3. The depth of the visible pits is in the range of 20 nm to 40 nm.

Although monolayer terraces are hardly visible in the AFM area map due to the chosen height contrast and their small height difference compared to the deep pits, they are present on the flat regions between the pits. A similar picture from the center of the wafer is shown in Fig. 4. The growth conditions in this area are Ga-rich and shallow hillocks are visible, which indicate a different decoration of defects during growth at slightly modified stoichiometry. The height of only a few atomic steps and the large lateral dimensions of the hillocks cause the roughness to be not significantly influenced. An atomically-smooth step flow pattern is revealed and emphasized in the line profile C in Fig. 4. Additionally, several tiny depressions are visible, sometimes aligned or on top of hillocks. For both cases, shown in Fig. 3 and Fig. 4, the density of deep pits or hillocks, respectively, is in the range of $2 \cdot 10^9 \text{ cm}^{-2}$ - $5 \cdot 10^9 \text{ cm}^{-2}$ and thus correlates well with the density of pits related to TSD or TMD of the used GaN template.

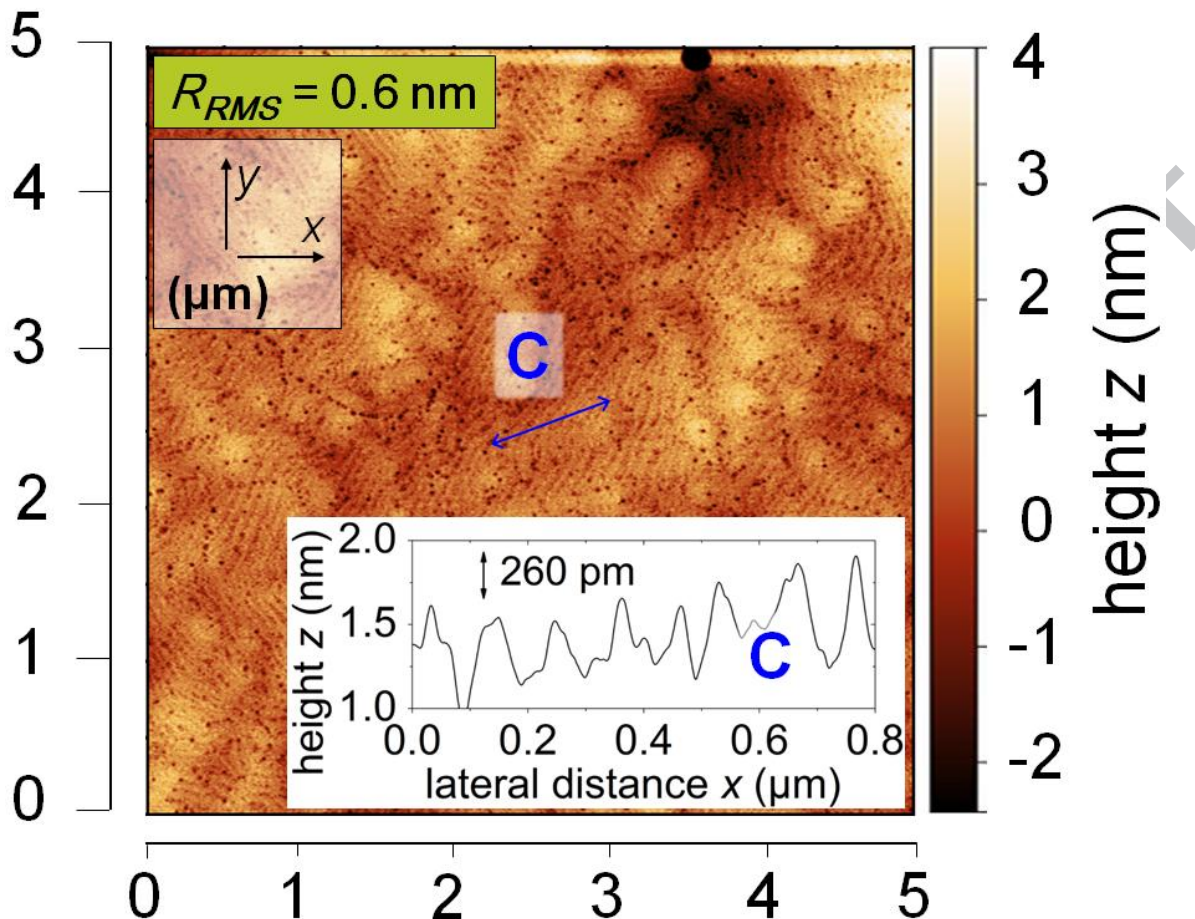


Fig. 4: Surface morphology and line scan profile C of an MBE overgrown layer stack under Ga-rich conditions taken from the center of the sapphire based structure. A terrace structure with monolayer high steps and hillock surface structures as well as small pits can be seen. The line scan profile C shows a selection with the typical small pits and atomic terraces. (These pits are located in the center of hillocks or in between and occasionally arranged in line-like formations.)

At this point, we conclude that the decoration of specific threading dislocations, i.e. deep pits or shallow hillocks, depends crucially on the III/N stoichiometry, but the density of these surface structures is determined by the density of TSD and TMD ending on the surface of the bare substrate. The generation of a significant amount of additional defects during MBE growth is not seen.

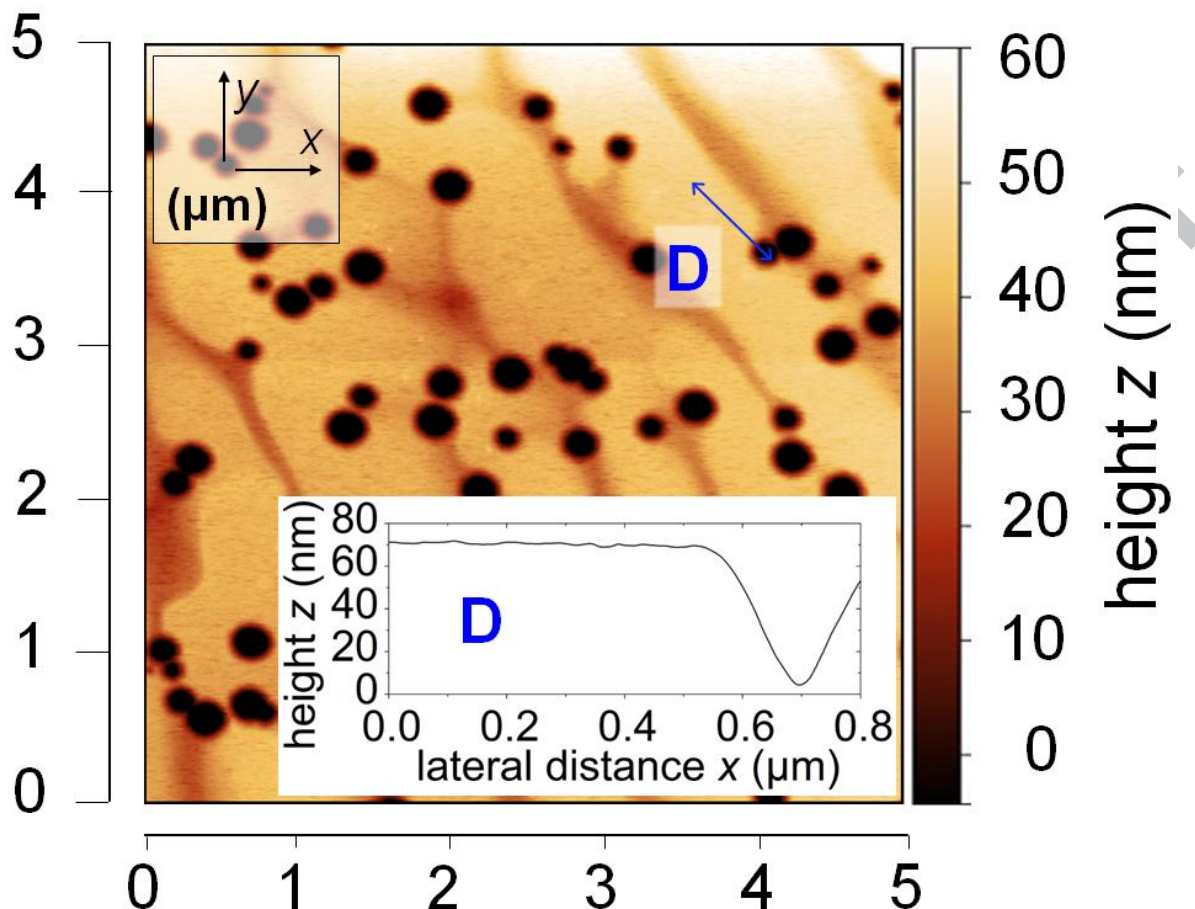


Fig. 5: Surface morphology and line scan profile D of a MBE overgrown layer stack under Ga-lean conditions on a sapphire based substrate with a dislocation density of $8 \cdot 10^8 \text{ cm}^{-2}$. The observable pits are 50 nm - 70 nm deep as can be seen in the line scan profile shown in the inset.

Empirically, on thicker templates less defects before and after MBE growth are expected. These expectations are validated when looking at the surface morphology of a heterostructure grown under Ga-lean conditions on a $90 \mu\text{m}$ thick HVPE GaN layer (Fig. 5). Pits with a depth of 50 nm - 70 nm and a density of $3 \cdot 10^8 \text{ cm}^{-2}$ are observed after MBE growth. For this particular template the density before the MBE procedure was not verified by AFM; instead we relied on the value of $1 \cdot 10^8 \text{ cm}^{-2}$ specified by the vendor. Two interpretations of the data seem feasible. First, during the MBE growth defects with a density in the range of $2 \cdot 10^8 \text{ cm}^{-2}$ are additionally generated. Or second, the specified density by the vendor was understated and only an insignificant number of defects is

added during the MBE procedure. To validate either of the interpretations the growth on a bulk GaN substrate with a much lower dislocation density was executed. The obtained data are presented and discussed in the following section.

3.2 Surface morphology of a heterostructure grown on bulk GaN

The next step was a heterostructure growth on a bulk GaN substrate with a vendor specified dislocation density of $< 5 \cdot 10^4 \text{ cm}^{-2}$. In Fig. 6 an AFM-image of the surface morphology of the AlGaIn/GaN heterostructure from the center of the wafer, where hillock-like surface structures should form around TSD or TMD, is shown. For a better description of the observed morphology the line profiles (E) are separately shown in Fig. 7 for two different directions representing the a- and m- axis of the hexagonal GaN crystal lattice. As seen from the line profiles the ripples (not visible on the epitaxy-ready surface before MBE overgrowth!) in Fig. 6 correspond to sub-nanometer steps. The determination of an actual step height is bound to the height-resolution limit of the used AFM, which is emphasized by an artifact at $y = 2.5 \text{ }\mu\text{m}$. Below this line the imaging resolution is deteriorated. Nevertheless steps of around once or twice the height of the single monolayer thickness (260 pm) can be discerned in the upper portion of the micrograph. The periodicity varies along the crystallographic a- and m-directions, which can be linked to the miscuts with respect to the c-direction. The miscut of 0.33° and 0.075° for the a- and m-axis, respectively, was verified by high-resolution x-ray diffraction measurements and matches the vendor-specified values. Hence, the surface morphology is purely given by the flat terrace structure of the 2D growth mode, which is imprinted by the miscut of the substrate.

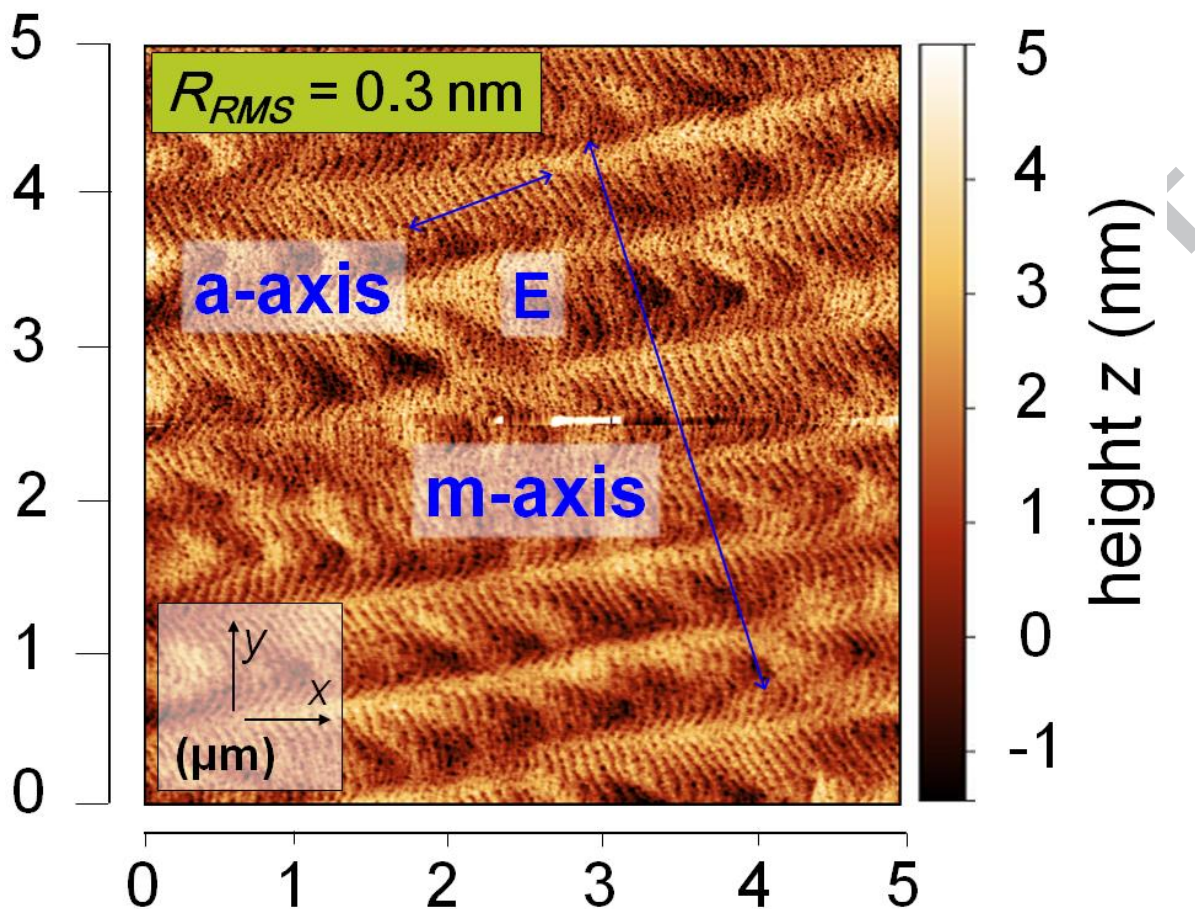


Fig. 6: Surface morphology of the MBE overgrown layer stack under Ga-rich conditions in the center of the bulk GaN substrate. Atomic monolayer high steps on the a-axis and corrugation on the m-axis of the crystal lattice can be observed matching the specified off-cut of the host substrate in the respective direction. The line scan profiles E are shown separately in Fig. 7.

The absence of any hillock-like surface feature in Fig. 6 leads to the conclusion that by MBE overgrowth only a very small amount of additional TSD or TMD could have been generated, but for sure much less than the discrepancy of $2 \cdot 10^8 \text{ cm}^{-2}$ between the measured pit-density in Fig. 5 and the vendor specification of the HVPE GaN on sapphire sample. This impressively manifests the high quality of the MBE homoepitaxy.

Furthermore no difference of the surface appearance in regions with varying stoichiometry (center/edge inhomogeneity) could be observed, just because the fingerprint of the dislocation-mediated surface structures e.g. hillocks or deep pits is missing in the $5 \times 5 \mu\text{m}^2$ images of the center or edge, respectively. Similar results were

found on Si-doped layers dedicated for vertical devices¹⁹, but just a more thorough statistical evaluation of samples with a defect density below around $1 \cdot 10^7 \text{ cm}^{-2}$ enables a quantifiable data evaluation.

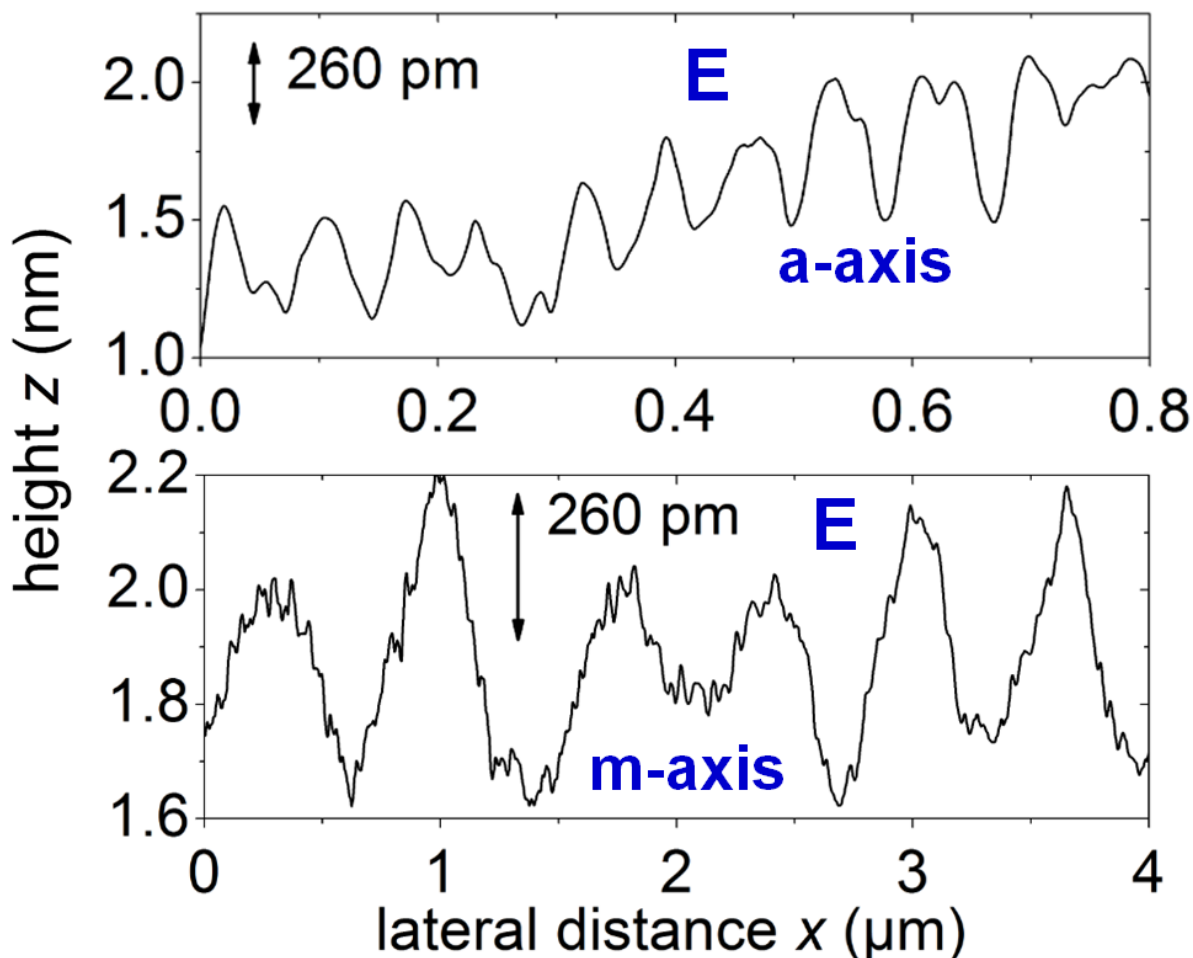


Fig. 7: Line scan profiles E with the height vs. lateral distance obtained from Fig. 6 in m- and a-axis direction of the crystal lattice. On both axis atomic mono and double layer high corrugation can be observed correlatable to the specified off-cut of the host substrate of 0.33° and 0.075° for a- and m-axis, respectively.

4. Summary and conclusion

The comparison of the surface morphology investigated by AFM of heterostructures grown by MBE on various sapphire-based and bulk GaN substrates underlines the importance of the III/N ratio for the decoration of crystal defects during the growth. Utilizing the inherently present fluctuation of the Ga-flux over the wafer the surface

morphology around specific types of dislocations can be varied in a segmented experiment in a single growth run. Although this defect decoration is strongly dependent on the III/N stoichiometry the defect concentration is set by the used substrate. On GaN substrates with low dislocation density and under Ga-rich growth conditions on sapphire-based substrates a surface roughness of below 0.6 nm was achieved. For all surfaces after the MBE growth a terrace step flow pattern was observed. However the decoration of defects by deep pits during a Ga-lean growth on a substrate with high defect density results in a strongly increased roughness unfavourable for further device processing and electrical operation. A high-quality heterostructure, which should be obtained by MBE overgrowth, thus necessarily demands a low dislocation density substrate. The observations made on bulk GaN substrates indicates that a low dislocation density of the substrate can be transferred in a high-quality MBE-grown heterostructure without creation of a noticeable amount of additional defects, though extended physical and statistical investigations would be necessary to fully confirm this finding. Additionally they reveal the translation of crystallographic information e.g. the miscut, from the host substrate surface to the surface of the overgrown MBE layers. Our experiments demonstrate a reliable nondestructive determination of the substrate TSD and TMD density after MBE growth (especially under Ga-lean conditions), which is not always trivial for pristine substrates.

Acknowledgements

This work was partially funded by the German Federal Ministry of Economics and Technology - BMWI (project no.: 03ET1398B) and by the German Ministry of Education and Research - BMBF (project no.: 16ES0145K).

References

- ¹ V. Kumar, A. Kuliev, T. Tanaka, Y. Otoki, and I. Adesida, *Electron. Lett.* **39**, 1758 (2003).
- ² Y. Cai, Y. Zhou, K.J. Chen, and K.M. Lau, *IEEE Electron Device Lett.* **26**, 435 (2005).
- ³ C.S. Suh, A. Chini, Y. Fu, C. Poblentz, J.S. Speck, and U.K. Mishra, in *2006 64th Device Res. Conf.* (2006), pp. 163–164.
- ⁴ M. Ishida, T. Ueda, T. Tanaka, and D. Ueda, *IEEE Trans. Electron Devices* **60**, 3053 (2013).
- ⁵ K.J. Chen, O. Häberlen, A. Lidow, C. I Tsai, T. Ueda, Y. Uemoto, and Y. Wu, *IEEE Trans. Electron Devices* **64**, 779 (2017).
- ⁶ T. Hashizume, K. Nishiguchi, S. Kaneki, J. Kuzmik, and Z. Yatabe, *Mater. Sci. Semicond. Process.* (2017).
- ⁷ Q. Zhou, Y. Yang, K. Hu, R. Zhu, W. Chen, and B. Zhang, *IEEE Trans. Ind. Electron.* **64**, 8971 (2017).
- ⁸ F. Schubert, U. Merkel, T. Mikolajick, and S. Schmult, *J. Appl. Phys.* **115**, 083511 (2014).
- ⁹ F. Schubert, S. Zybell, J. Heitmann, T. Mikolajick, and S. Schmult, *J. Cryst. Growth* **425**, 145 (2015).
- ¹⁰ J.W.P. Hsu, M.J. Manfra, S.N.G. Chu, C.H. Chen, L.N. Pfeiffer, and R.J. Molnar, *Appl. Phys. Lett.* **78**, 3980 (2001).
- ¹¹ E.J. Tarsa, B. Heying, X.H. Wu, P. Fini, S.P. DenBaars, and J.S. Speck, *J. Appl. Phys.* **82**, 5472 (1997).
- ¹² R.J. Molnar, W. Götz, L.T. Romano, and N.M. Johnson, *J. Cryst. Growth* **178**, 147 (1997).
- ¹³ J.L. Weyher, S. Lazar, L. Macht, Z. Liliental-Weber, R.J. Molnar, S. Müller, V.G.M. Sivel, G. Nowak, and I. Grzegory, *J. Cryst. Growth* **305**, 384 (2007).
- ¹⁴ S. Schmult, F. Schubert, S. Wirth, A. Großer, T. Mittmann, and T. Mikolajick, *J. Vac. Sci. Technol. B Nanotechnol. Microelectron. Mater. Process. Meas. Phenom.* **35**, 02B104 (2017).
- ¹⁵ F. Schubert, S. Wirth, F. Zimmermann, J. Heitmann, T. Mikolajick, and S. Schmult, *Sci. Technol. Adv. Mater.* **17**, 239 (2016).
- ¹⁶ M.J. Manfra, K.W. Baldwin, A.M. Sergent, R.J. Molnar, and J. Caissie, *Appl. Phys. Lett.* **85**, 1722 (2004).
- ¹⁷ M.J. Manfra, S.H. Simon, K.W. Baldwin, A.M. Sergent, K.W. West, R.J. Molnar, and J. Caissie, *Appl. Phys. Lett.* **85**, 5278 (2004).
- ¹⁸ B. Heying, E.J. Tarsa, C.R. Elsass, P. Fini, S.P. DenBaars, and J.S. Speck, *J. Appl. Phys.* **85**, 6470 (1999).
- ¹⁹ R. Hentschel, S. Schmult, A. Wachowiak, A. Großer, J. Gärtner, and T. Mikolajick, *J. Vac. Sci. Technol. B Nanotechnol. Microelectron. Mater. Process. Meas. Phenom.* **36**, 02D109 (2018).

- defect-free MBE growth of functional GaN/AlGaN heterostructures on bulk GaN
- nondestructive surface defect evaluation by AFM before and after MBE growth
- the surface defect density after MBE growth is limited by the substrate quality
- defect decoration as pits or hillocks depending on the III/N stoichiometry

ACCEPTED MANUSCRIPT